Trapped mesoscopic quantum gas in a magnetic field

2000 J. Phys. A: Math. Gen. 33 1857

(http://iopscience.iop.org/0305-4470/33/9/310)

J. Phys. A: Math. Gen. **33** (2000) 1857–1871. Printed in the UK PII: S0305-4470(00)10522-0

Trapped mesoscopic quantum gas in a magnetic field

P N Vorontsov-Velyaminov, R I Gorbunov and S D Ivanov
Faculty of Physics, St Petersburg University, 198904 St Petersburg, Russia

Received 22 December 1999

Abstract. Feynman-type series for grand potential Ω, number of particles, internal energy, magnetization and susceptibility are derived for systems of noninteracting quantum particles in an external magnetic field. Numerical calculations at constant N for harmonically trapped systems of fermions and bosons in the presence of a homogeneous magnetic field are carried out with the aid of both Feynman-type series and series over single-particle states. N-convergence to universal curves for chemical potential and energy is presented. At low temperatures magnetization of the Fermi gas exhibits a pronounced quantum behaviour.

1. Introduction

In [1] we have shown that cycle series presentation of the grand canonical potential Ω introduced initially by Feynman for the Bose gas in a box [2] can be extended to systems of noninteracting bosons or fermions with a spin in an arbitrary external field. Coefficients in this series can be expressed through a single-particle canonical partition function at increasing values of inverse temperature. For an exactly solvable Schrödinger problem (e.g., in the case of harmonic field or Pöschl–Teller potential [3, 4]) the single-particle canonical partition function is determined and hence the potential Ω and related averages can be easily calculated numerically. We considered our results mainly in a methodological aspect, i.e. as providing reliable exact data for checking our PIMC calculations for quantum systems of interacting particles [5, 6]. Meanwhile, experiments on trapped mesoscopic systems at superlow temperatures [7–10] as well as a series of recent theoretical and numerical studies (e.g. [11–35]) point to a more or less direct application of results obtained for ideal Bose and Fermi systems.

In this paper we extend our previous study to systems in a magnetic field. Although in the most general case, i.e. for an inhomogeneous magnetic field, the Hamiltonian of the system does not split into coordinate and spin parts, the Feynman-type expression for the potential Ω still holds due to the absence of interaction between particles. We consider in detail an example of harmonically trapped quantum gas in the presence of a homogeneous magnetic field when the single-particle Schrödinger problem has an exactly determined energy spectrum. This makes it possible to construct a single-particle canonical partition function which enters into Ω. The expression for Ω is then used for obtaining series for the number of particles, internal energy and magnetization. Magnetic susceptibility is considered in the appendix. Purely paramagnetic, diamagnetic and general cases of Bose and Fermi systems are then investigated numerically. In calculations we use Feynman-type series in regions where $\mu < 0$ and conventional series over single-particle states in the whole range of μ.

0305-4470/00/091857+15$30.00

2. General approach

2.1. Feynman-type series

The starting point is the standard form for the canonical partition function of a system of N identical particles [2]:

$$Z^{(S,A)}(\beta) = \frac{1}{N!}\sum_{\{P\}} \xi^{[P]} Z^{(D)}(\beta; P) \tag{1}$$

where (S, A) and $\xi = \pm 1$ stand for symmetric and antisymmetric cases respectively, (D) corresponds to a system of distinguishable particles, P denotes permutation, $[P]$ its parity and $\beta \equiv T^{-1}$.

In the case of noninteracting quantum particles with a spin in an inhomogeneous magnetic field the Hamiltonian cannot be separated into purely spin and coordinate terms and hence $Z^{(D)}(\beta)$ does not split into a product either, as in the absence of magnetic field considered in [1]. However, the Hamiltonian is still a sum of single-particle terms, $\hat{H} = \sum_{i=1}^{N} \hat{H}_1(i)$, due to the absence of interaction, and hence

$$\rho(\boldsymbol{x}, \boldsymbol{x}'; \beta) = \langle \boldsymbol{x} | \mathrm{e}^{-\beta \hat{H}} | \boldsymbol{x}' \rangle = \prod_{i=1}^{N} \rho_1(x_i, x_i{}'; \beta). \tag{2}$$

Here x_i is a set of single-particle variables for the ith particle including coordinates and spin, $\rho_1(x_i, x_i{}'; \beta) = \langle x_i | \mathrm{e}^{-\beta \hat{H}_1(i)} | x_i' \rangle$ is the related density matrix, $\boldsymbol{x} = (x_1, x_2, \ldots, x_N)$. $\rho(\boldsymbol{x}, \boldsymbol{x}'; \beta)$ is the N-particle density matrix yielding $Z^{(D)}(\beta; P)$:

$$Z^{(D)}(\beta; P) = \int \rho(\boldsymbol{x}, P\boldsymbol{x}; \beta)\, \mathrm{d}\boldsymbol{x}. \tag{3}$$

Further analysis is close to that of [1]. Consider that variables (x_i) of the first ν particles in the P permutation are involved in a cycle yielding an independent factor in $Z^{(D)}(\beta; P)$:

$$Z_\nu(\beta) = \int \rho_1(x_1, x_2; \beta)\rho_1(x_2, x_3; \beta) \ldots \rho_1(x_\nu, x_1; \beta) \prod_{i=1}^{\nu} \mathrm{d}x_i. \tag{4}$$

Hence $Z^{(D)}(\beta; P)$ is expressed as a product of such independent terms:

$$Z^{(D)}(\beta; P) = \prod_{\nu=1}^{N} Z_\nu(\beta)^{C_\nu(P)} \tag{5}$$

where $C_\nu(P)$, a number of cycles of the length ν, satisfies the condition:

$$\sum_{\nu=1}^{N} \nu C_\nu(P) = N. \tag{6}$$

For $Z^{(S,A)}(\beta)$ in (1) we obtain

$$Z^{(S,A)}(\beta) = \frac{1}{N!}\sum_{\{P\}} \prod_{\nu=1}^{N} [\xi^{(\nu-1)} Z_\nu(\beta)]^{C_\nu(P)} \tag{7}$$

where we used a relation [1,2]: $[P] = \sum_\nu (\nu - 1) C_\nu(P)$.

Now following Feynman [2] (see also [1,36]) we arrive at an expression for the grand potential Ω:

$$\beta\Omega^{(S,A)}(\beta, \mu) = -\sum_{\nu=1}^{\infty} \frac{f_\nu}{\nu} \qquad f_\nu = \xi^{(\nu-1)} Z_\nu(\beta) \lambda^\nu. \tag{8}$$

For coefficients $Z_\nu(\beta)$ determined in (4) the following relation proved in [1] holds:

$$Z_\nu(\beta) = Z_1(\nu\beta). \tag{9}$$

Thus all the coefficients in (8) are expressed through a single-particle canonical partition function for increasing values of inverse temperature, $\nu\beta$.

We shall also need expression for Ω in terms of the single-particle energy spectrum ε_K (K stands for a set of single-particle state quantum numbers):

$$\beta\Omega(\beta,\mu) = \xi \sum_K \ln(1 - \xi\lambda \mathrm{e}^{-\beta\varepsilon_K}). \tag{10}$$

There is a close relation between forms (8) and (10) for Ω. Actually, expanding the logarithm function in (10) (note that it can be carried out only when $\lambda < 1$) and changing the order of summation in two series, the latter form for Ω can be transformed into the series over ν (8) [1] with $Z_\nu(\beta) = Z_1(\nu\beta) = \sum_K \mathrm{e}^{-\nu\beta\varepsilon_K}$.

2.2. Averages

Appropriate operations applied to Ω in forms (8) or (10) yield averages.

The number of particles:

$$N = -\left(\frac{\partial\Omega}{\partial\mu}\right)_\beta = \sum_{\nu=1}^{\infty} f_\nu \qquad f_\nu \equiv \xi^{\nu-1} Z_1(\nu\beta)\lambda^\nu \tag{11}$$

$$N = \sum_K n_K \qquad n_K \equiv \frac{1}{\mathrm{e}^{\beta(\varepsilon_K-\mu)} - \xi}. \tag{12}$$

Internal energy:

$$E = \frac{\partial}{\partial\beta}(\beta\Omega)_\mu + \mu N = -\sum_{\nu=1}^{\infty} f_\nu \left.\frac{\partial \ln Z_1(x)}{\partial x}\right|_{x=\nu\beta} \tag{13}$$

$$E = \sum_K n_K \varepsilon_K. \tag{14}$$

Magnetization:

$$M = -\frac{\partial\Omega}{\partial B} = \sum_{\nu=1}^{\infty} \frac{f_\nu}{\nu} \frac{\partial \ln Z_1(\nu\beta)}{\partial B} \tag{15}$$

$$M = -\sum_K n_K \frac{\partial\varepsilon_K}{\partial B}. \tag{16}$$

3. Homogeneous magnetic field

3.1. Energy eigenvalues

In the case of a homogeneous magnetic field, $\vec{B} = (0, 0, B)$, the single-particle Hamiltonian is a sum of coordinate and spin parts, $\hat{H}_1 = \hat{H}_1^{sp} + \hat{H}_1^c$ where $\hat{H}_1^{sp} = -\frac{e\hbar}{mc} B\hat{s}_z$, $\hat{s}_z$ is the spin projection operator with eigenvalues σ, $|\sigma| \leqslant s$, s being the spin of a particle. For electrons, $s = \frac{1}{2}$, $\sigma = \pm\frac{1}{2}$. $\hat{H}_1^c$, in its turn, can be presented as a sum of transverse and longitudinal parts: $\hat{H}_1^c = \hat{H}_{1\perp}^c(B) + \hat{H}_{1\|}^c$, where the latter does not depend on B. So the Schrödinger equation splits into three independent equations, and eigenvalues of $\hat{H}_1$ can be presented as

$$\varepsilon_K \Rightarrow \varepsilon_{\vec{k},\sigma} = \varepsilon_\sigma + \varepsilon_{k_\perp} + \varepsilon_{k_\|}. \tag{17}$$

$\varepsilon_\sigma = -2\mu_B B\sigma$, where $\mu_B \equiv \frac{e\hbar}{2mc}$ is the Bohr magneton. $\varepsilon_{k_\parallel}$ is an eigenvalue of a one-dimensional equation for the longitudinal (z) component. In a number of cases (e.g., for harmonic or Pöschl–Teller potentials) it has an exact solution.

The transverse equation is a two-dimensional one and includes magnetic field. In the presence of an additional isotropic harmonic field its Hamiltonian is

$$\hat{H}^c_{1\perp}(B) = \frac{1}{2m}\left(\hat{\vec{p}} - \frac{e}{c}\vec{A}\right)^2 + \frac{m\omega^2(x^2+y^2)}{2} \tag{18}$$

where $\hat{\vec{p}}$ is a two-dimensional vector-operator of momentum and the vector potential, $\vec{A}$, also lacks z-component since $\vec{A} \perp \vec{B}$. Choosing it as $\vec{A} = \frac{[\vec{B}\vec{r}]}{2}$ and introducing polar coordinates one arrives at an equation which has an exact solution with energy eigenvalues presented as [37]:

$$\varepsilon_{k_\perp} \Rightarrow \varepsilon_{l,n} = (2n + |l| + 1)\hbar\tilde{\omega} - l\frac{\hbar\omega_c}{2} \tag{19}$$

with $n = 0, 1, 2, \ldots$; $l = 0, \pm 1, \pm 2, \ldots$; $\omega_c = \frac{eB}{mc}$ is the cyclotron frequency, $\tilde{\omega} = \sqrt{\omega^2 + (\frac{\omega_c}{2})^2}$ and ω is the frequency of the harmonic field.

If in the transverse (x, y) directions the system is limited by hard walls no exact solution is known and one can use a quasiclassical approximation with a g-fold degenerate energy spectrum [38, 39]:

$$\varepsilon_{k_\perp} \Rightarrow \varepsilon_j = \frac{e\hbar B}{mc}\left(j + \frac{1}{2}\right). \tag{20}$$

$g = \frac{S}{2\pi}\frac{eB}{\hbar c}$ and S is an area of the walls' cross section with the (x, y)-plane (the form of the cross section does not affect the spectrum, see also [23]).

3.2. *Harmonically trapped system*

For a quantum particle with a spin in an isotropic harmonic field plus homogeneous magnetic field the energy eigenvalues are determined as

$$\varepsilon_{\sigma kln} = -2\mu_B B\sigma + (k + \tfrac{1}{2})\hbar\omega + \varepsilon_{l,n} \tag{21}$$

where $|\sigma| \leqslant s$; $k = 0, 1, \ldots$; and $\varepsilon_{l,n}$ is determined in (19).

The related canonical partition function which enters Ω-potential (8) can be presented as a product of spin, longitudinal and transverse factors:

$$Z_1 = Z_1^{sp} Z_{1\parallel} Z_{1\perp} \tag{22}$$

where the spin contribution is

$$Z_1^{sp} = \sum_{|\sigma|\leqslant s} \mathrm{e}^{2\beta\mu_B B\sigma}. \tag{23}$$

For spinless particles $Z_1^{sp} = 1$, in the absence of magnetic field $Z_1^{sp} = 2s + 1$, for electrons, $s = \frac{1}{2}$, $Z_1^{sp} = 2ch(\beta\mu_B B)$.

$Z_{1\parallel}$ is a partition function for a one-dimensional oscillator:

$$Z_{1\parallel} = \frac{1}{2\mathrm{sh}(\frac{\beta\hbar\omega}{2})}. \tag{24}$$

For $Z_{1\perp}$ we can write:

$$Z_{1\perp} = \sum_{0\leqslant n<\infty} \mathrm{e}^{-\beta\hbar\tilde{\omega}(2n+1)} \sum_{-\infty<l<\infty} \mathrm{e}^{-\beta\hbar(\tilde{\omega}|l| - l\omega_c/2)}. \tag{25}$$

The sum over n yields $(\mathrm{e}^{\beta\hbar\tilde{\omega}} - \mathrm{e}^{-\beta\hbar\tilde{\omega}})^{-1}$ while the sum over m can be easily reduced to

$$1 + \frac{1}{\mathrm{e}^{\beta\hbar\omega_+} - 1} + \frac{1}{\mathrm{e}^{\beta\hbar\omega_-} - 1} \tag{26}$$

where $\omega_\pm = \tilde{\omega} \pm \frac{\omega_c}{2}$. Combining both expressions we finally obtain for $Z_{1\perp}$:

$$Z_{1\perp} = \frac{1}{2\mathrm{sh}(\frac{\beta\hbar\omega_+}{2})} \frac{1}{2\mathrm{sh}(\frac{\beta\hbar\omega_-}{2})}. \tag{27}$$

This result (together with (24)) coincides with that of relation (3.4) in [28] where it was obtained as a trace of the appropriate propagator. So the coordinate part of the canonical partition function (Z_1^c) for a particle in an isotropic oscillator field in the presence of a homogeneous magnetic field appears to be that for a three-dimensional anisotropic oscillator with frequencies ω, ω_+, ω_-, the latter two being dependent on magnetic field B. Note that $\omega_+\omega_- = \omega^2$.

Expression (22) for Z_1 with (23), (24), (27) for Z_1^{sp}, $Z_{1\parallel}$ and $Z_{1\perp}$ is now inserted into Ω (8) and averages N (11), E (13) and M (15).

For E we get

$$E = \sum_{\nu=1}^{\infty} f_\nu \left(-\mu_B B \mathrm{th}(\nu\beta\mu_B B) + \frac{\hbar\omega}{2}\mathrm{cth}\frac{\nu\beta\hbar\omega}{2} + \frac{\hbar\omega_+}{2}\mathrm{cth}\frac{\nu\beta\hbar\omega_+}{2} + \frac{\hbar\omega_-}{2}\mathrm{cth}\frac{\nu\beta\hbar\omega_-}{2} \right). \tag{28}$$

For M we get

$$M = \sum_{\nu=1}^{\infty} f_\nu M_\nu \qquad M_\nu \equiv \mu_B \mathrm{th}(\nu\beta\mu_B B) - \frac{e\hbar}{2mc}\frac{1}{2}\left(\frac{\omega_+}{\tilde{\omega}}\mathrm{cth}\frac{\nu\beta\hbar\omega_+}{2} - \frac{\omega_-}{\tilde{\omega}}\mathrm{cth}\frac{\nu\beta\hbar\omega_-}{2} \right). \tag{29}$$

In order to obtain Ω, N and E in terms of the series over single-particle states one needs simply to substitute $\varepsilon_{\sigma kln}$ from (21) into (10), (12) and (14) for ε_K. M is obtained from (16):

$$M = \sum_{\sigma kln} n_{\sigma kln} M_{\sigma kln} \qquad M_{\sigma kln} \equiv \left(2\mu_B\sigma - \frac{e\hbar}{2mc}\left((2n + |l| + 1)\frac{\omega_c}{2\tilde{\omega}} - l \right) \right). \tag{30}$$

Expressions for magnetic susceptibility are too long so we present them in the appendix. The high-temperature limit of zero-field susceptibility is obtained there as well.

4. Numerical calculations

4.1. Computational scheme

The computational scheme that we use here mostly follows that of [1]. Series (11) or (12) for N as a function of β, B and μ are treated as equations for determining $\mu(\beta)|_{B=const}$ dependences at N fixed. These, in their turn, are inserted into (28), (14) and (29), (30) to get $E(\beta, B)$ and $M(\beta, B)$ at constant N. In calculations of μ-, E- and M-dependences on N, values of β and B were fixed, while for getting the corresponding dependence on B we fixed β and N.

In our calculations, similarly to [1], we count the chemical potential from the ground state. It implies that a combination $\varepsilon_K - \mu$ which enters exponents in both series is presented as $\varepsilon_K - \varepsilon_0 - (\mu - \varepsilon_0)$ where ε_0 is the ground state energy and a substitution is made: $\mu - \varepsilon_0 \Rightarrow \mu$. For systems in a harmonic trap with a homogeneous magnetic field, $\varepsilon_0 = \frac{\hbar}{2}(\omega + \omega_+ + \omega_-) - 2\mu_B Bs$.

While making calculations we can separately consider a purely paramagnetic case (a model of 'uncharged particles' with $s \neq 0$), a purely diamagnetic case (a model of 'spinless charged particles', $s = 0$) and the general case with complete account for magnetic interactions in (11), (28), (29) or (12), (14), (30). In the first 'pure case' one needs to make a formal substitution: $\frac{e\hbar}{2mc} \Rightarrow 0$, $\omega_c \Rightarrow 0$ while, in the second, $\mu_B \Rightarrow 0$ in all the above relations.

Feynman-type series are one-dimensional ones and hence are the most convenient for computations. Unfortunately, they cannot be used in regions where $\mu > 0$, i.e. for fermions at low temperatures. Series over single-particle states are three-dimensional and the number of terms to be taken into account to achieve the desired accuracy is much greater than in cases with series over cycles.

In calculations with the second series in the absence of a magnetic field we truncate when the value of the last term becomes less than a certain δ [1]. On switching on the magnetic field it was found that the series ceases to be monotonic. This made us change both the order of summation and the truncation condition. The accuracy of our calculations varies in the range of $\delta = 10^{-5}$–10^{-8} dependent on the set of input parameters.

The convergence of cycle series is much faster than for the second one even at low temperatures (provided $\mu < 0$). Thus for bosons at $T < 0.1$ ($\hbar\omega$ units) the number of terms to be accounted for in the cycle series, 10^5, is ten times less than for the second series. For cycle series the required number of terms strongly decreases with the increase of temperature while for the second one it continues to grow. So, for bosonic systems we could use cycle series in the whole range of temperatures.

4.2. Temperature dependences

Butts and Rokhsar [11] point to a fact that the $\mu(T)$ dependence in continuous spectrum approximation for fermions in a harmonic field can be presented by a universal curve (figure 1 in [11], see also [13]). Following a similar line we obtain universal curves for $\mu(T)$ and $E(T)$ for both systems and present our numerical data at various fixed N in an appropriate scale for comparison.

In a continuous energy spectrum approximation the expression (12) for fermions with spin s in an anisotropic harmonic field with frequencies $\omega_1, \omega_2, \omega_3$ and in the absence of magnetic field yields

$$N = \int_0^\infty \frac{g(\varepsilon)\,\mathrm{d}\varepsilon}{\mathrm{e}^{\beta(\varepsilon-\mu)} + 1} \tag{31}$$

with $g(\varepsilon) = \frac{(2s+1)\varepsilon^2}{2\hbar^3\omega_1\omega_2\omega_3}$. The Fermi energy in continuous spectrum approximation is $\varepsilon_F^0 = \hbar(\omega_1\omega_2\omega_3)^{1/3}(\frac{6N}{2s+1})^{1/3}$.

Now scaling all parameters and variable ε in (31) by ε_F^0 we arrive at an expression which lacks N:

$$1 = 3\int_0^\infty \frac{x^2\,\mathrm{d}x}{\mathrm{e}^{b(x-\tilde{\mu})} + 1} \tag{32}$$

where $x \equiv \varepsilon/\varepsilon_F^0$, $b \equiv \beta\varepsilon_F^0 = (T/\varepsilon_F^0)^{-1}$, $\tilde{\mu} \equiv \mu/\varepsilon_F^0$.

The desired universal dependence $\tilde{\mu}(T/\varepsilon_F^0)$ is obtained numerically from (32).

In a similar way one gets a universal curve for the scaled internal energy:

$$\frac{E}{N\varepsilon_F^0} = 3\int_0^\infty \frac{x^3\,\mathrm{d}x}{\mathrm{e}^{b(x-\tilde{\mu})} + 1}. \tag{33}$$

The integral is calculated as a function of scaled temperature, T/ε_F^0, and of the previously obtained $\tilde{\mu}(T/\varepsilon_F^0)$ dependence.

For bosons an appropriate scaling parameter is $T_c = \hbar(\omega_1\omega_2\omega_3)^{1/3}(\frac{N}{\zeta(3)(2s+1)})^{1/3}$, the temperature of Bose condensation in continuous spectrum approximation (see, e.g., [1,21,24]):

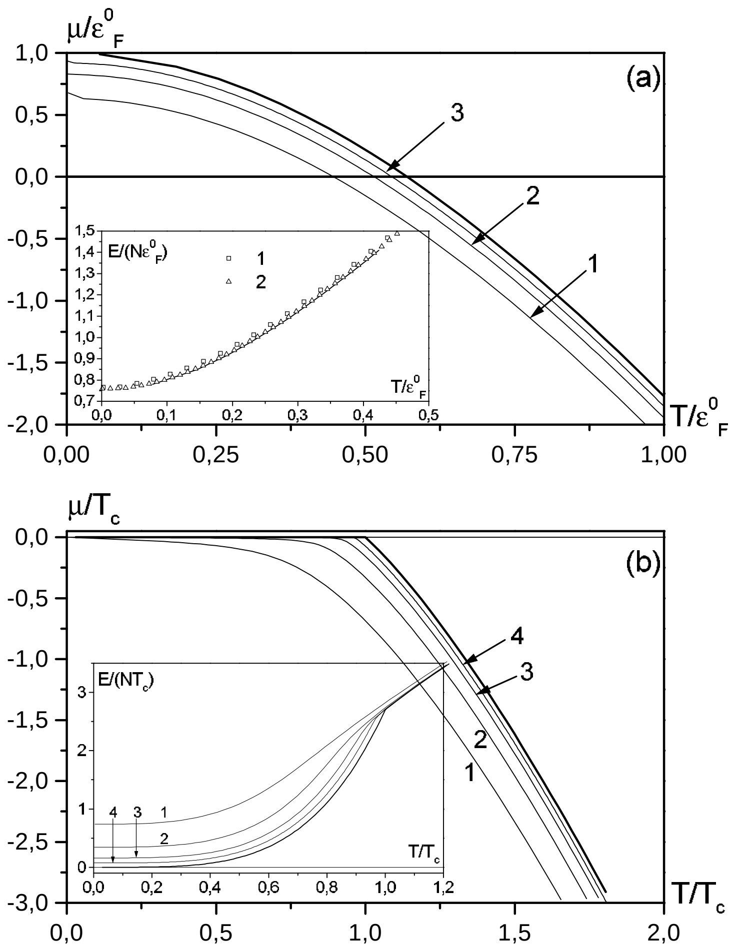

Figure 1. Scaled temperature dependences [1] of chemical potential and internal energy (inset) for systems of N particles in a 3D isotropic harmonic field. (a) Fermions, curves 1–3 are for values of $\frac{N}{2s+1} = 10$, 100, 1000. (b) Bosons, curves 1–4 are for $\frac{N}{2s+1} = 10, 100, 10^3, 10^4$. Universal curves are shown by thick curves.

$\zeta()$ is the ζ-function, $\zeta(3) = 1.202$. So universal curves for $\mu(T)$ and $\frac{E}{NT_c}$ are

$$1 = \zeta(3)^{-1} \int_0^\infty \frac{x^2\,\mathrm{d}x}{\mathrm{e}^{b(x-\tilde{\mu})} - 1} \tag{34}$$

$$\frac{E}{NT_c} = \zeta(3)^{-1} \int_0^\infty \frac{x^3\,\mathrm{d}x}{\mathrm{e}^{b(x-\tilde{\mu})} - 1} \tag{35}$$

where $x \equiv \varepsilon/T_c$, $b \equiv \beta T_c = (T/T_c)^{-1}$, $\tilde{\mu} \equiv \mu/T_c$ for $T \geqslant T_c$ and $\tilde{\mu} = \mu = 0$ for $T \leqslant T_c$.

Scaling implies presentation of our $\mu(T)$ and $E(T)$ numerical dependences for fixed N in ε_F^0 (or in T_c) units as well as change of T-scale, $T \Rightarrow T/\varepsilon_F^0$ (or $T \Rightarrow T/T_c$).

Such scaling of our previous results for systems in an isotropic harmonic field [1] is shown in figures 1(a) and (b). Convergence to limiting universal curves with the increase of N is well observed. It is especially fast for the energy of fermions.

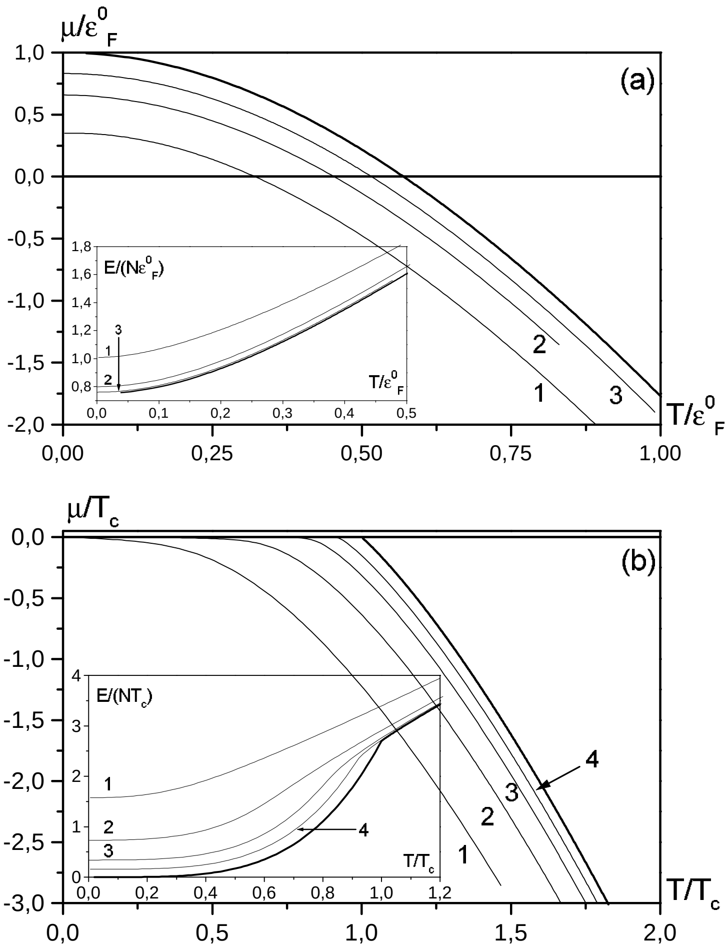

Figure 2. Scaled temperature dependences of chemical potential and internal energy (inset) for systems of N particles in a 3D harmonic field plus magnetic field, for the purely diamagnetic case ($s = 0$), $\omega_c/\omega = 5$. (*a*) Fermions, curves 1–3 are for values of $N = 10$, 100, 1000. (*b*) Bosons, curves 1–4 are for $N = 10$, 100, 10^3, 10^4; Universal curves are the thick curves.

In the presence of the magnetic field we can expect a similar N-convergence for a purely diamagnetic system; in this case increasing of the magnetic field is equivalent to the increase of anisotropy of the oscillator field. Note, also, that although frequencies ω_+ and ω_- depend on B their product holds constant, $\omega\omega_+\omega_- = \omega^3$, so the 'effective volume' of the trap does not depend on B.

In order to check the influence of the magnetic field we made calculations for a single value of N ($N = 10$) and a set of increasing values of magnetic field B (actually at fixed ω_c/ω) in the purely diamagnetic case. For bosons, the increase of ω_c/ω results in a monotonic deviation of curves from that for $B = 0$. In the interval $0 \leqslant \omega_c/\omega \leqslant 1$ the effect is extremely small while for higher values of ω_c/ω it becomes much greater. Similar features are observed also for the energy of fermions. For the chemical potential of fermions, on the contrary, changes are great in the whole range of ω_c/ω and the shift of curves with the increase of magnetic field is nonmonotonic.

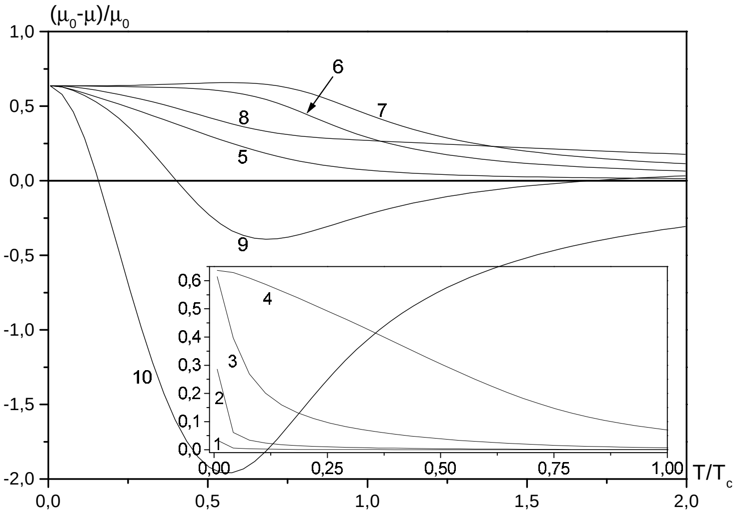

Figure 3. Relative deviation of chemical potential versus temperature for bosons ($N = 10$, $s = 1$) at increasing ω_c/ω. Curves 1–4 are for $\omega_c/\omega = 10^{-4}, 10^{-3}, 10^{-2}, 0.1$. (inset); curves 5–10 are for $\omega_c/\omega = 0.1, 0.5, 1.0, 5.0, 10.0, 25.0$. μ_0 is the chemical potential in the absence of a magnetic field.

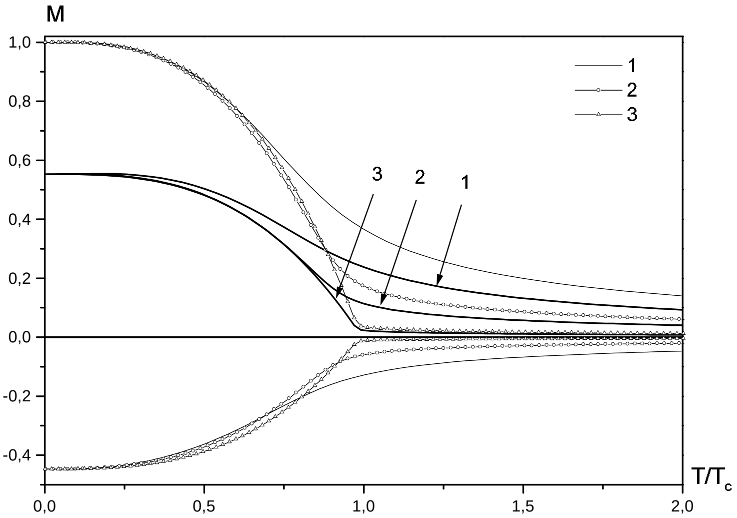

Figure 4. M versus T dependence for bosonic system, $s = 1$, in magnetic field $\omega_c/\omega = 1$: curves 1–3 are for $N = 10, 100, 10^4$. Thick curves are for complete magnetization, other curves, above and below zero, are for the paramagnetic and diamagnetic contributions respectively.

To observe N-convergence for data at constant ω_c/ω we choose the value $\omega_c/\omega = 5.0$, for which the effect of the magnetic field is already great in all cases considered above. In figure 2 we see a monotonic N-convergence to the universal curves in qualitative accordance with the results of figure 1.

Similar dependences at $\omega_c/\omega = 5.0$ in the general case, i.e. when we simultaneously account for both magnetic interactions, showed that N-convergence to the universal curves still holds.

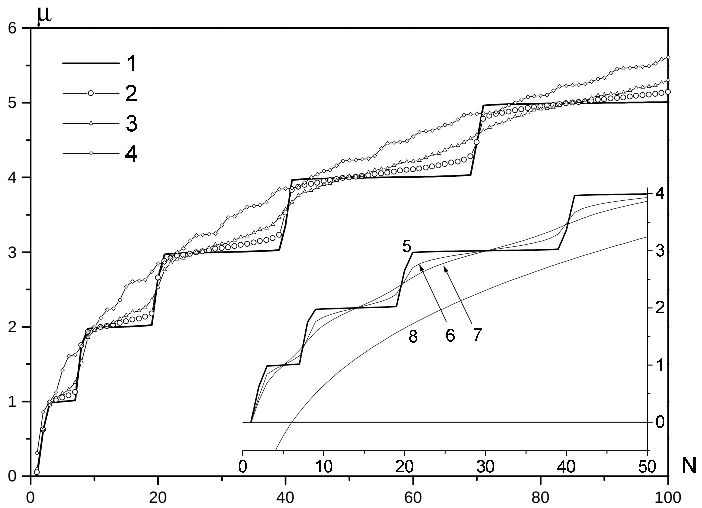

Figure 5. μ versus N dependences for fermions, $s = \frac{1}{2}$, in a 3D isotropic harmonic field at constant T. At $T = 0.01$ with magnetic field, curves 1–4 correspond to $\omega_c/\omega = 0, 0.1, 0.2, 1.0$. In the absence of a magnetic field (inset), curves 5–8 correspond to a set of temperatures $T = 0.01, 0.1, 0.2, 1.0$; μ and T are in $\hbar\omega$ units.

At low temperatures the chemical potential for bosonic systems is very close to zero. So in order to check clearly the effect of the magnetic field it is convenient to present it as the relative difference $(\mu - \mu_0)/\mu_0$ versus T/T_c for increasing values of ω_c/ω, figure 3 ($N = 10$, $s = 1$, complete account for magnetic interaction). At very low ω_c/ω (10^{-4}–10^{-1}), inset, the dependences are monotonic with initial values increasing from 0.04 up to 0.64. Further increase of ω_c/ω does not change this initial value while the whole dependency is changed in a rather particular way from curve 6 for $\omega_c/\omega = 0.1$ to curve 10 for $\omega_c/\omega = 25.0$.

Temperature dependences of magnetization of bosons, $s = 1$, with a complete account for magnetic interaction at $\omega_c/\omega = 1.0$ and for a set of N, is shown in figure 4. Indicated are complete values together with their paramagnetic and diamagnetic contributions. Curves strongly resemble those for magnetics at a phase transition with the 'critical temperature' $T/T_c = 1$. Increase of N results in a sharpening of the curves in the vicinity of this point.

It should be kept in mind that the presented data are obtained from the grand canonical expressions and can be treated only as 'pseudocanonical'. This can differ greatly from true canonical data in the vicinity of the Bose condensation point, as follows from paper [16] of Balazs and Bergeman.

4.3. *Low-temperature data for fermions*

In a recent paper [12], Schneider and Wallis demonstrated an interesting behaviour of chemical potential and other properties as functions of T and N for a system of harmonically trapped spinless fermions at $T \ll 1$ (T is in $\hbar\omega$ units). Thus at $T = 0.002$, $\mu(N)$-dependence has a pronounced stepwise character caused by a shell structure of energy levels in a 3D isotropic harmonic field: this structure is determined by the degeneracy factor $g(\varepsilon_k) = \frac{(k+1)(k+2)}{2}$. The steps in the obtained staircase correspond to completely filled $1, 2, 3, \ldots$ shells with $N = 1, 4, 10, 20, 35, 56, \ldots$ for spinless fermions (or twice that numbers for $s = \frac{1}{2}$). The height of each step equals to 1 (in $\hbar\omega$ units).

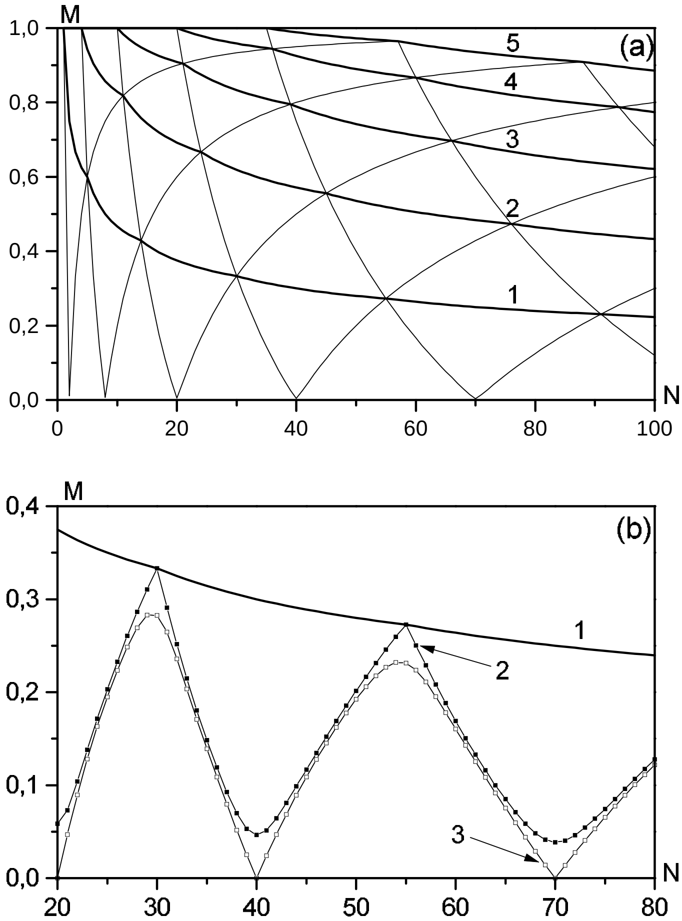

Figure 6. Specific magnetization M versus N dependence at fixed magnetic field for fermions, $s = \frac{1}{2}$, in the purely paramagnetic case, $T = 0.01$ ($\hbar\omega$ units). (*a*) General outlook, curves 1–5 correspond to integer values of $\omega_c/\omega = 1, 2, 3, 4, 5$; zigzag lines below curve 1, between curves 1 and 2, etc, are for intervals of $\omega_c/\omega = 0.05$–0.95, 1.05–1.95 etc, respectively; (*b*) presents a fragment of (*a*) with curves 1–3 corresponding to $\omega_c/\omega = 1.0, 0.95, 0.05$. The zigzag line of the first order should occupy a narrow strip between curves 2 and 3 and is not presented. M is in μ_B units.

For a system of fermions, $s = \frac{1}{2}$, at $T = 0.01$ we reproduced the stepwise N-dependence for μ and its evolution (smoothing of steps up to their final decay) with increasing temperature observed in [12] in the absence of magnetic field, see the inset to figure 5. Similar calculations were performed at increasing values of magnetic field (figure 5). The rise of magnetic field at $T = 0.01$ also smooths the steps up to their destruction.

For a better understanding of the phenomena occurring in the system at low temperatures in the presence of a magnetic field we made a number of calculations of specific magnetization M, either as a function of N at constant B (at fixed ratio ω_c/ω) or as a function of B (of ω_c/ω) for fixed N. We consider the purely paramagnetic case ('uncharged fermions' with $s = \frac{1}{2}$), the purely diamagnetic case ('charged spinless fermions') and the general case with inclusion of both effects into (30). In the general case, magnetization can be separated into paramagnetic and diamagnetic contributions.

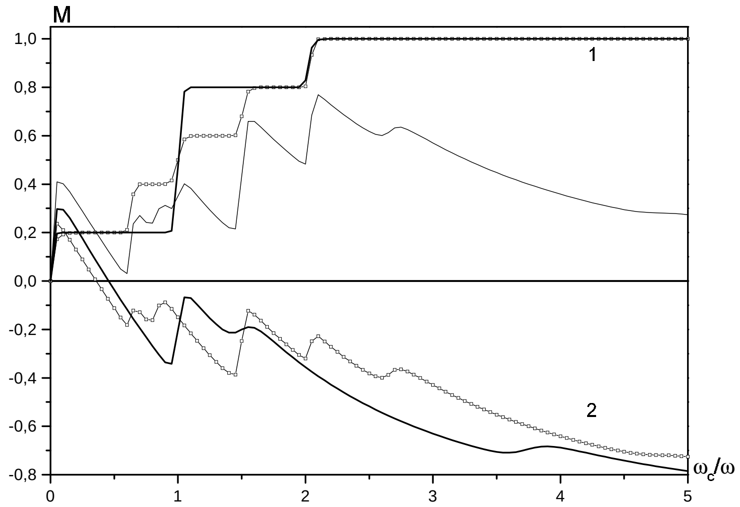

Figure 7. Specific magnetization M versus magnetic field (ω_c/ω) dependences for a fixed number of particles. $T = 0.01$, $N/(2s+1) = 5$: thin curve is for the general case $(s = \frac{1}{2})$, squares are for its paramagnetic and diamagnetic contributions (1 and 2), thick curves are for the purely paramagnetic $(s = \frac{1}{2})$ and diamagnetic $(s = 0)$ cases (1 and 2); M is in μ_B units.

The N-dependence of M at $T = 0.01$ and gradually increasing values of ω_c/ω, ranging from 0 to 5 for the purely paramagnetic case is shown in figure 6. The $M(N)$ dependences are presented by zigzag lines of the first, second, third, etc orders, separated by smooth curves which correspond to integer values of ω_c/ω: $0, 1, 2, \ldots$. The zigzag of the first order corresponds to values of ω_c/ω approximately in the range of 0.05–0.95; the second, in the range 1.05–1.95, etc. This can be easily understood from figure 6(*b*) where a fragment of the whole diagram (figure 6(*a*)) is shown with lines 2, 3 corresponding to $\omega_c/\omega = 0.05, 0.95$. The zigzag of the first order is located in a narrow strip between these lines and is omitted in the figure 6(*b*). Another important feature is that points of its intersection with the N-axis $(M = 0)$ are the 'magic numbers', i.e. populations of completely filled shells mentioned above: $2, 8, 20, 40, 70, \ldots$ for $s = \frac{1}{2}$.

Low-temperature isotherms $(T = 0.01)$ of M for $N = 10$ as functions of magnetic field are presented in figure 7. First of all we see that paramagnetic and diamagnetic contributions into the mixed case do not coincide with those for pure cases, which are also shown in figure 7. Hence the combined action of two factors included into magnetic interaction is not reduced to a simple sum. The change in M due to paramagnetic effect in both pure and mixed cases is a stepwise monotonic increase of M in the range of $0 < \omega_c/\omega < 2$. For the purely paramagnetic case jumps occur at $\omega_c/\omega = 0, 1, 2$. Magnitudes of jumps are equal to $0.2, 0.6, 0.2$, which corresponds to consecutive reorientation of a spin in the outer (noncompleted) shell with two fermions, then three spins of the filled shell of six, and finally the last spin of two occupying the internal filled shell. The diamagnetic part in both cases is a nonmonotonic dependency of almost linear decreases alternating with stepwise up-jumps occupying the same range of ω_c/ω. Increase of temperature $(N = 10, T = 0.1)$ resulted in a considerable smoothing of the dependences of figure 7. For greater values of N the general picture is principally the same, although the range of M-oscillations widens and their structure becomes more complicated.

5. Final remarks

We have extended a Feynman-type presentation of the grand potential Ω for a system of noninteracting quantum particles with spin to a case of external magnetic field. Exact expressions have been derived for harmonically trapped systems in a homogeneous magnetic field. A computational scheme mostly following our previous work [1] has been applied for high accuracy calculations of $\mu(\beta, B)$-dependences at constant number of particles N which, in turn, have been used to calculate internal energy E and magnetization M as functions of β, B and N. Feynman-type series as well as series over single-particle states were used. Temperature dependences for fermionic and bosonic gases are presented in a scaled form and a convergence to universal curves for $\mu(\beta)$ and $E(\beta)$ at fixed B are observed. Low-temperature data for fermionic systems in purely paramagnetic or diamagnetic cases as well as in the general case of complete account of magnetic interactions exhibit a stepwise or oscillatory behaviour which is smoothed down as the temperature increases. The applied approach seems to be promising for obtaining other accurate data for trapped finite systems of noninteracting quantum particles in an external magnetic field for a wide range of parameters.

In cases when the spectrum is unknown, quasiclassical approximation can be used in calculating series over single-particle states.

Acknowledgment

This work has been supported by the Russian Foundation of Fundamental Research, Grant 99-02-16774.

Appendix

To get the magnetic susceptibility we start with an expression:

$$\chi = \frac{\partial M}{\partial B}. \tag{A.1}$$

Substituting (29) into (A.1) we obtain

$$\begin{aligned} \chi &= \sum_{\nu=1}^{\infty}\left(\frac{\partial f_\nu}{\partial B}M_\nu + f_\nu\frac{\partial M_\nu}{\partial B}\right) \equiv \chi_1^{(1)} + \chi_2^{(1)} \\ \chi_1^{(1)} &\equiv \beta\sum_{\nu=1}^{\infty}\nu f_\nu M_\nu^2 \qquad \chi_2^{(1)} \equiv \sum_{\nu=1}^{\infty} f_\nu \frac{\partial M_\nu}{\partial B}. \end{aligned} \tag{A.2}$$

For $\chi_2^{(1)}$ we arrive at an expression:

$$\begin{aligned} \chi_2^{(1)} = \beta\sum_{\nu=1}^{\infty}\nu f_\nu\Bigg\{\frac{\mu_B^2}{\mathrm{ch}^2(\nu\beta\mu_B B)} - \frac{1}{4}\left(\frac{e\hbar}{2mc}\right)^2\Bigg[\left(\frac{\omega}{\tilde\omega}\right)^2\frac{2}{\nu\beta\hbar\tilde\omega}\left(\mathrm{cth}\frac{\nu\beta\hbar\omega_+}{2} + \mathrm{cth}\frac{\nu\beta\hbar\omega_-}{2}\right) \\ -\left(\left(\frac{\omega_+}{\tilde\omega}\right)^2\frac{1}{\mathrm{sh}^2(\frac{\nu\beta\hbar\omega_+}{2})} + \left(\frac{\omega_-}{\tilde\omega}\right)^2\frac{1}{\mathrm{sh}^2(\frac{\nu\beta\hbar\omega_-}{2})}\right)\Bigg]\Bigg\}. \end{aligned} \tag{A.3}$$

In the absence of magnetic field $\chi_1^{(1)}$ vanishes and $\chi_2^{(1)}$ yields

$$\chi_2^{(1)}|_{B=0} = \beta\mu_B^2\sum_{\nu=1}^{\infty}\nu f_\nu - \frac{\beta}{2}\left(\frac{e\hbar}{2mc}\right)^2\sum_{\nu=1}^{\infty}\nu f_\nu\left[\frac{2}{\nu\beta\hbar\omega}\mathrm{cth}\left(\frac{\nu\beta\hbar\omega}{2}\right) - \frac{1}{\mathrm{sh}^2(\frac{\nu\beta\hbar\omega}{2})}\right]. \tag{A.4}$$

Applying (A.1) to (30) we obtain χ in the form of a series over single-particle states:

$$\chi = \sum_{\sigma kln} \left(\frac{\partial N_{\sigma kln}}{\partial B} M_{\sigma kln} + N_{\sigma kln} \frac{\partial M_{\sigma kln}}{\partial B} \right) = \chi_1^{(2)} + \chi_2^{(2)}. \tag{A.5}$$

For $\chi_1^{(2)}$ and $\chi_2^{(2)}$ we get

$$\chi_1^{(2)} \equiv \beta \sum_{\sigma kln} N_{\sigma kln}^2 \mathrm{e}^{\beta(\varepsilon_{\sigma kln} - \mu)} M_{\sigma kln} \tag{A.6}$$

$$\chi_2^{(2)} \equiv -2 \left(\frac{e\hbar}{2mc} \right)^2 \frac{1}{\hbar\tilde{\omega}} \frac{\omega^2}{\tilde{\omega}^2} \sum_{\sigma kln} N_{\sigma kln}(2n + |l| + 1). \tag{A.7}$$

In the absence of magnetic field $\chi_1^{(2)} = 0$ and $\chi_2^{(2)}$ yields

$$\chi_2^{(2)}|_{B=0} = -2 \left(\frac{e\hbar}{2mc} \right)^2 \frac{1}{\hbar\omega} \sum_{\sigma kln} N_{\sigma kln}(2n + |l| + 1) \tag{A.8}$$

with $\varepsilon_{\sigma kln}|_{B=0} = (k + 2n + |l| + \frac{3}{2})\hbar\omega$ in $N_{\sigma kln}$ (12).

Finally, we present the high-temperature limit of the zero field susceptibility obtained from (A.4) and including paramagnetic and diamagnetic terms respectively:

$$\left. \frac{\chi}{N} \right|_{\substack{B=0 \\ \beta \to 0}} = \chi_0 = \mu_B^2 \beta - \left(\frac{e\hbar}{2mc} \right)^2 \frac{\beta}{3}. \tag{A.9}$$

So, a relation $\chi_0^{dia} = -\frac{1}{3}\chi_0^{para}$ [39] holds in our case (see also [38]).

References

[1] Vorontsov-Velyaminov P N, Ivanov S D and Gorbunov R I 1999 *Phys. Rev.* E **59** 168
[2] Feynman R P 1972 *Statistical Mechanics* (New York: Benjamin)
[3] Pöschl G and Teller E 1933 *Z. Phys.* **83** 143
[4] Flügge S 1971 *Practical Quantum Mechanics* (Berlin: Springer)
[5] Vorontsov-Velyaminov P N, Nesvit M O and Gorbunov R I 1997 *Phys. Rev.* E **55** 1979
[6] Lyubartsev A P and Vorontsov-Velyaminov P N 1993 *Phys. Rev.* A **48** 4075
[7] Anderson M H, Ensher J R, Matthews M R, Weiman C E and Cornell E A 1995 *Science* **269** 198
[8] Bradley C C, Sackett C A, Tollett J J and Hulet R G 1995 *Phys. Rev. Lett.* **75** 1687
[9] Davis K B, Mewes M-O, Andrews M R, van Druten N J, Durfee D S, Kurn D M and Ketterle W 1995 *Phys. Rev. Lett.* **75** 3969
[10] Pinkse P W H, Mosk A, Weidemüller M, Reynolds M W, Hijmans T W and Walrafen J T M 1998 *Phys. Rev.* A **57** 4747
[11] Butts D A and Rokhsar D S 1997 *Phys. Rev.* A **55** 4346
[12] Schneider J and Wallis H 1998 *Phys. Rev.* A **57** 1233
[13] Li M, Yan Z, Chen J, Chen L and Chen C 1998 *Phys. Rev.* A **58** 1445
[14] Bruun G M and Burnett K 1998 *Phys. Rev.* A **58** 2427
[15] Terra M O, Tiago M L and de Aguiar M A M 1998 *Phys. Rev.* E **58** 5146
[16] Balazs N L and Bergeman T 1998 *Phys. Rev.* A **58** 2359
[17] Grossmann S and Holthaus M 1997 *Phys. Rev. Lett.* **79** 3557
[18] Herzog C and Olshanii M 1997 *Phys. Rev.* A **55** 2427
[19] Gaida M and Rzazewski K 1997 *Phys. Rev. Lett.* **78** 2686
[20] Navez P, Bitouk D, Gaida M, Idziaszek Z and Rzazewski K 1997 *Phys. Rev. Lett.* **79** 1789
[21] Patria R K 1998 *Phys. Rev.* A **58** 1490
[22] Baym G and Pethick C J 1996 *Phys. Rev. Lett.* **76** 6
[23] Kirsten K and Toms D J 1999 *Phys. Rev.* E **59** 158
[24] Haugset T, Haugerud H and Andersen J O 1997 *Phys. Rev.* A **55** 2922
[25] Lee M H 1997 *Phys. Rev.* E **55** 1518
[26] Patria R K 1998 *Phys. Rev.* E **57** 2697

[27] Apostol M 1997 *Phys. Rev.* E **56** 4854
[28] Brosens F, Devreese J T and Lemmens L F 1997 *Phys. Rev.* E **55** 227
[29] Brosens F, Devreese J T and Lemmens L F 1997 *Phys. Rev.* E **55** 6795
[30] Brosens F, Devreese J T and Lemmens L F 1998 *Phys. Rev.* E **57** 3871
[31] Grüter P, Ceperley D and Laloë F 1997 *Phys. Rev. Lett.* **79** 3549
[32] Pearson S, Pang T and Chen C 1998 *Phys. Rev.* A **58** 1485
[33] Pearson S, Pang T and Chen C 1998 *Phys. Rev.* A **58** 4796
[34] Pearson S, Pang T and Chen C 1998 *Phys. Rev.* A **58** 4811
[35] Krauth W 1996 *Phys. Rev. Lett.* **77** 3695
[36] Elliot J P and Dawber P G 1979 *Symmetry in Physics* (London: Macmillan)
[37] Galitskij V M, Karnakov B M and Kogan V I 1992 *Problems in Quantum Mechanics* (Moscow: Nauka) p 79 problem 7.5 (in Russian)
[38] Huang K 1963 *Statistical Mechanics* (New York: Wiley)
[39] Landau L D and Lifshitz E M 1995 *Statistical Physics* (Moscow: Nauka) (in Russian)